Applied Catalysis B: Environmental 128 (2012) 135–143

Contents lists available at SciVerse ScienceDirect

Applied Catalysis B: Environmental

journal homepage: www.elsevier.com/locate/apcatb

Glycerol as a probe molecule to uncover oxidation mechanism in photocatalysis

Claudio Minero*, Andrea Bedini, Valter Maurino

Dipartimento Chimica Analitica, Università degli Studi di Torino, via Pietro Giuria 5, 10125 Torino, Italy

ARTICLE INFO

Article history:
Available online 24 February 2012

Keywords:
Glycerol
Photocatalysis
Fluorination
Shallow traps
OH radical

ABSTRACT

Glycerol is a good probe molecule to understand what type of photocatalytic mechanism could occur at the catalyst surface, as the analysis of the produced intermediates is able to discriminate between a direct electron transfer and a radical mediated oxidation mechanism. The mechanism of transformation of glycerol is explored by an extensive analysis of formed intermediates as a function of glycerol concentration on two different commercial TiO_2 powders. Over TiO_2 Degussa P25 the transformation rate of glycerol shows a sharp maximum as a function of the substrate concentration. The type of product detected at low glycerol concentration (glyceraldehyde and dihydroxyacetone) changes after the sharp maximum giving mainly formaldehyde and glycolaldehyde. On Merck TiO_2, characterized by a lower density and more uniform population of hydroxyls at surface sites, mainly glyceraldehyde and dihydroxyacetone are observed. Because these products are formed through an •OH-like mechanism, the products observed on P25 derive from a direct electron transfer. The results are rationalized invoking the surface complex of glycerol where an inner sphere electron transfer occurs, which leads to glycerol fragmentation, and where the substrate-mediated recombination plays the major role. A simplified kinetic approach confirms the observed rate dependence on concentration.

The working hypothesis is also confirmed by addition of fluoride anions that compete for surface sites and impede glycerol complexation. Without the possibility of inner sphere electron transfer, on P25 only glyceraldehyde and dihydroxyacetone are observed. Thus different catalysts differ for the possibility of surface complexation.

1. Introduction

The photocatalytic glycerol transformation was previously investigated [1] due to the large interest in the raw biodiesel glycerol conversion [2–4]. In the preliminary investigation on the glycerol transformation [1] emerged that the selectivity among C_3 (glyceraldehyde + dihydroxyacetone (1,3-dihydroxy-2-propanone)) and $C_2 + C_1$ products (formaldehyde and glycolaldehyde) were present only on P25. The selectivity was dependent on glycerol concentration. Other interesting features were the unusual rate dependence on glycerol concentration, with a sharp maximum, over Degussa P25 TiO_2, and the more usual increasing behaviour over Merck TiO_2 and on both fluorinated TiO_2s.

It is not new that the two titania powders exhibit different chemical behaviour. For example, hydroxyl groups on the surface of hydrated TiO_2 P25 are able to transform benzaldehyde molecules in hemiacetalic-like surface species, whereas C_6H_5CHO molecules are only weakly perturbed by interaction with the OH groups on TiO_2 Merck [5].

The activity and selectivity of the photocatalytic process are complex function of several catalyst properties, including crystallinity, surface area, surface morphology, nature of the surface hydroxyl groups, substrate and cation/anion adsorption [6,7]. Moreover, the kinetic of the process depends on the substrate concentration, due to a complex interplay between substrate oxidation and substrate-mediated carrier recombination (back reactions) [8], reactor geometry and particle scattering [9].

The published data on particles morphology suggest a good uniformity of the TiO_2 Merck particle surfaces and a more defective surface for the P25 particles [5]. In a more recent paper [10] we reported by a comparative FT-IR analysis under various conditions the presence of a variety of surface OH on P25, that is at least 3 types of linear hydroxy groups (in which OH is bound to a surface Ti, let say ≡Ti—OH), and 3 types of bridged hydroxy groups (≡Ti—OH—Ti≡). There is a large consensus on the action of surface hydroxyls as surface hole traps, so their chemical nature is relevant to photocatalysis. The trapped holes (and electrons) are less reactive than their bulk photogenerated precursors, although reaction of free carriers with surface chemisorbed molecules can be very rapid and efficient [11,12].

Fluorination of P25 greatly simplifies the surface IR spectrum, leaving only the component at 3674 cm^{-1} that was assigned to

* Corresponding author. Tel.: +39 011 6705293; fax: +39 011 6705242.
E-mail address: claudio.minero@unito.it (C. Minero).

0926-3373/$ – see front matter © 2012 Elsevier B.V. All rights reserved.
doi:10.1016/j.apcatb.2012.02.014

one type of bridged hydroxy groups. It is long known that fluoride adsorbs onto TiO_2 surfaces (see for example [13]), and the adsorption of fluoride inhibits the adsorption of other ligands, e.g. catechol and hydrogen peroxide [6]. The νOH components removed by fluorination can be ascribed to hydroxyls sitting on defective sites, which interact more strongly with ligands. The surface of TiO_2 P25 is characterized by the presence of at least two different hydroxyls, with different coordination strength toward fluorides (and presumably to other ligands). The confirmation of this picture comes from the evolution of νOH patterns for TiO_2 Merck and their comparison with P25. Pristine and fluorinated Merck TiO_2 show similar νOH pattern, with a dominant spectroscopic feature at 3674 cm^{-1}. The effect of fluorination in this case is the decrease of the intensity at 3674 cm^{-1}, but the pattern does not change. The spectra of pristine and fluorinated Merck TiO_2 are very similar to that of fluorinated P25. In fact, the partial data on rates measured on fluorinated P25 [1] (with most adsorption sites masked) are very similar to that on fluorinated and pristine Merck, except for a factor 4–5 higher that was ascribed to the different surface area of catalysts.

The rate dependence of the rate on the glycerol concentration cannot be explained with current kinetic models based on Langmuir–Hinshelwood assumptions [14,15] or that embody only one active site like the majority of kinetic models and particularly by those that do not allow for back reactions, i.e. substrate mediated charge carrier recombination, that were recognized as essential for rate interpretation [8,9,16]. Papers published by Ollis and co-workers [17,18] pointed out the need of a two site model to explain the partial deactivation observed in the gas phase degradation of alcohols and aromatics over P25 TiO_2, without presenting evidences about the nature of these two sites, but only asserting the presence of a Type I site, suitable for the adsorption of substrate (actually aromatics), water and reaction intermediates, and a Type II more hydrophilic (hydroxyl groups or bridging oxygen) site unsuitable for substrate adsorption.

All the evidences reported above suggest the presence of different sites on the surface of the two catalysts, which play a key role on the kinetic behaviour. The peculiar molecular structure of glycerol, a symmetric molecule with two lateral and equivalent hydroxyl groups, that when undergoes oxidation leads to glyceraldehyde, and one central hydroxyl group that after oxidation leads to dihydroxyacetone (C_3 compounds), or can fragment in two non-equivalent parts (formaldehyde + glycolaldehyde, $C_1 + C_2$ compounds) prompted us to perform a full kinetic study of evolution of these compounds on P25 and Merck TiO_2, either pristine or fluorinated, with the aim of elucidating the role of TiO_2 surface active sites and clarifying the nature of involved reactive species.

2. Experimental

General details of the irradiation procedure and sample preparation is reported in the previous paper [1]. The irradiation experiments were carried out in Pyrex glass (cut-off at 295 nm) cylindrical cells (4.0 cm diameter, 2.3 cm height), containing 5 mL of the aqueous suspension of the photocatalyst powder and substrate, using a Philips TL K 05 fluorescent lamp. This lamp emits a band 30 nm wide, centred at 360 nm. The total photonic flux in the cell was 3.45×10^{-7} einstein min^{-1} (ferrioxalate actinometry). Size and morphology of the TiO_2 microcrystals are available [5]. The TiO_2 powders (Degussa P25, 80% anatase, 20% rutile, mean particle size 40 nm, BET surface area 50 $m^2 g^{-1}$, and Merck for analysis, 100% anatase, mean particle size 140 nm, BET surface area 10 $m^2 g^{-1}$) were purified from organic and ionic impurities by irradiation and washing. After irradiation, the suspensions were filtered through 0.45 μm membranes (cellulose acetate, Millipore HA) and analysed for glycerol (GLY) and other hydroxylated

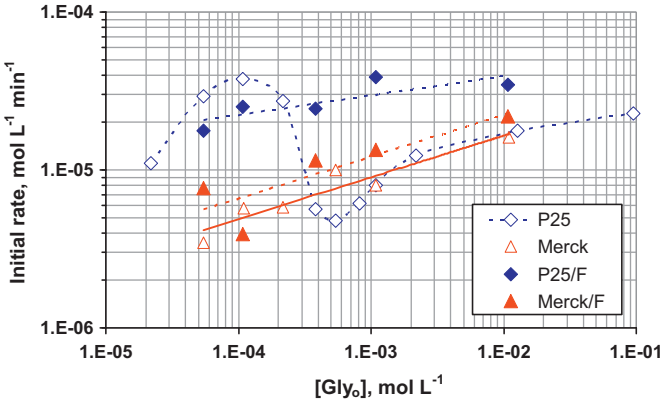

Fig. 1. Initial photocatalytic transformation rates of glycerol as a function of the glycerol concentration over pristine (pH 5.5) and fluorinated (pH 3.0, total fluoride concentration 10 mM) TiO_2 catalysts (0.5 g L^{-1}).

products (dihydroxyacetone (DHA), glyceraldehyde (GAD), glycolaldehyde (GLC) and formaldehyde (FORM)). Detection of glycerol was performed as before [1] with a Dionex DX 500 ion chromatograph equipped with an ED40 electrochemical detector operated in the integrated amperometry mode and a CarboPac MA1 Analytical Column (Dionex, 250 mm length, 4 mm diameter). The detection was performed with a three-step waveform optimized for the detection of hydroxyl groups. Reproducibility of analytical procedure was evaluated on pure standards at different concentrations and resulted ±3%. Symbols used in figures (see later) are larger than this uncertainty.

The detection of hydroxylated intermediates was improved with respect to the previous work to separate GAD from DHA and to increase the sensitivity. The derivatization was carried out as follows: 1.0 mL of the irradiated and filtered slurry is mixed with 0.250 mL of (2,4-dinitrophenyl)hydrazine solution in ACN (1.5 g L^{-1}) and 0.100 mL of 2.0 M phosphoric acid aqueous solution. The mixture is allowed to stand for 30 min, then directly analysed by HPLC. Reproducibility of the procedure was evaluated on pure standards and resulted ±5%. The separation was performed with a Hitachi LaChrom Elite liquid chromatograph equipped with a high pressure L-2130 pump, a L-2200 autosampler, a L-2300 oven and a L-2455 DAD. A RP C18 column Pursuit^{TM} XRs Ultra 2.8 Varian (100 mm × 2 mm, 2.8 μm packing) was used and elution was carried out in isocratic condition with a ternary eluent (72% water, 18% THF and 10% ACN) at 0.4 mL/min. An example of the obtained chromatograms is reported in Fig. SI 1.

The experimental time profiles for the glycerol disappearance (and dihydroxyacetone and glyceraldehyde when starting from these pure compounds) followed pseudo-first order kinetic for at least two half lives. Because the kinetic analysis (see below) will be based on *initial* conversion rates, we restrict our fitting to less than one half life. For raw data analysis, the fit to an exponential decay function or to a first order kinetic is used merely to obtain a more robust evaluation of initial rates and does not imply any assumption on kinetic. Accumulation of degradation products and the change in kinetic regime observed at low substrate concentration can distort the time profiles at high conversions.

3. Results and discussion

The rates of glycerol disappearance were partially reported in ref. [1]. Those results, implemented with some new data are reported in Fig. 1 in a logarithmic scale, to be compared with the following kinetic analysis. Although the pristine and fluorinated sets are not at the same pH, the effect of pH at acidic pH is small, as the rate merely decreases of 13% by passing from pH 3.0 to 5.5

for P25 (see Table 2 in ref. [1]). The main evidence is the unusual rate dependence on substrate concentration for P25 and the small effect of fluorination on Merck TiO_2. Interestingly, after the sudden decrease at 0.4–0.5 mM glycerol, the rate for P25 is similar to that of Merck TiO_2, irrespective of the larger surface area of the former.

The scope of the present work was the assessment of intermediate evolution as the glycerol concentration is changed. Some characteristic time profile for Merck and P25 are compared in Fig. 2; all the raw data are reported in Figs. SI 2–4. Considering the time profiles of several intermediates at different initial glycerol concentrations for TiO_2 Merck reported in Fig. SI 2, the main products of phototransformation on TiO_2 Merck are the two C_3 carbohydrates GAD and DHA, produced from glycerol with relative ratio ranging from 1.3 to 1.8. Only at the larger concentrations of glycerol, glycolaldehyde (GLC) and formaldehyde (FORM) are produced together with a lower production of DHA. Formaldehyde can be formed also as product of DHA degradation or from the concurrent mechanism that is operating for P25 also at low concentration (see below).

On the contrary, main reaction products on TiO_2 P25 (see Fig. SI 3 and Fig. 2) depend on glycerol concentration. At low concentration GAD and DHA are formed in a relative ratio about 2, together with FORM and GLC. As the glycerol concentration increases and glycerol rate is strongly depressed (see insets) the main products are FORM and GLC. GAD and DHA are significantly present only before the rate fall at low glycerol concentrations (0.02 and 0.1 mM). Traces of GAD are detected at the larger glycerol concentration.

The evolution of intermediates when fluoride ions are added to the slurry is reported in Fig. SI 4 and Fig. 2. The evident experimental result is that mainly the two C_3 carbohydrates GAD and DHA are produced from glycerol in the presence of fluorides. On Merck TiO_2 almost no change is observed, whilst on P25 the production of GLC and FORM is strongly depressed. Fluoride is a good complexing agent for Ti(IV) cation, inhibiting the adsorption of substrates and causing several changes both in kinetics and in the oxidative mechanisms [6]. It was shown that surface complexation by the redox inactive fluoride anion leads to an increase of the transformation rate of organic substrates that react mainly through •OH radical mediated pathway, with a bell shaped dependence on pH, reflecting the surface distribution of ≡Ti—F. It was also reported on fluorinated P25 a sustained photoproduction of H_2O_2 [19]. The H_2O_2 production rate follows the TiO_2 surface speciation, showing a maximum at pH/concentration at which the surface coverage by ≡Ti—F is almost complete. The presence of fluoride ions inhibits the surface complexation of superoxides/peroxide species as ≡Ti—OO•, derived from the e_{CB} reduction of O_2, and then in turn inhibits the H_2O_2 degradation and the possibility of back reaction on ≡Ti—OO• sites.

As fluorides impede the surface complexation on the surface ≡Ti—OH site, the formation of GLC + FORM is strictly connected with GLY chemisorption. Then the surface complex ≡Ti—O—CH_2—CH(OH)—CH_2OH must be responsible of formation of $C_2 + C_1$ compounds. Attempts to measure the adsorption isotherm were not successful on pristine P25. In the presence of 10 g L^{-1} of P25 TiO_2, on average more than 98–99% of the GLY added concentration has been recovered in solution, indicating that the concentration of adsorbing sites (C_s (moles of sites L^{-1}) = $C_{cat} \times N_s$ where N_s is the number of sites g^{-1} and C_{cat} is given in g L^{-1}) is very low and/or the adsorption constant is $<1/C_s$.

The different observed types of products depend on the nature of the oxidizing species involved in the glycerol oxidation mechanism. The different pathways stem from the ability of the oxidant to cause one or multi electron transfer, or to abstract H atoms. Concerning the reactivity toward OH radical, reported kinetic constants are in the diffusive limit ($k = 2.0 \times 10^9$ L mol^{-1}) [20]. Identified oxidation products in the presence of Fenton reagents were dihydroxyacetone (DHA) and glyceraldehyde (GAD) [21,22]. The same products

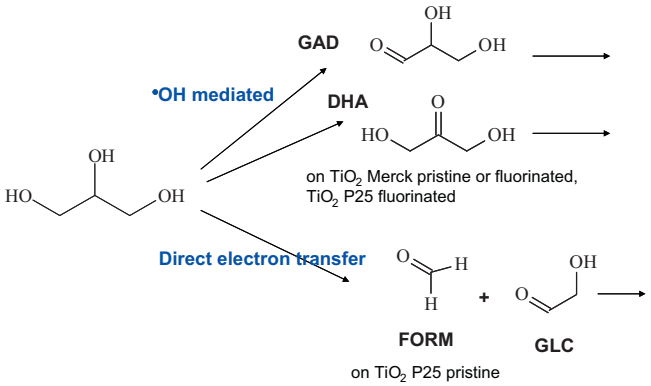

Scheme 1. Kinetic pathways for transformation of glycerol.

and the same ratio [GAD]/[DHA] are observed generating OH radicals through H_2O_2 photolysis. A detailed investigation of the kinetic of glycerol oxidation by H_2O_2 under UV will be reported elsewhere. Conversely, it is long known that vicinal diols undergo oxidative C—C cleavage with periodate, generating two carbonyl compounds [23,24]. Periodate is a strong oxidant ($E_{IO^{4-}/IO^{3-}} = 1.60$ V) acting through a bielectron transfer mechanism. Interestingly, oxidation mechanism proceeds through a formation of a cyclic diester between periodate and the vicinal diol. This type of mechanism can be relevant due to the ability of Ti(IV) to form complexes with polyhydroxylated compounds [25]. In the case of ethylene glycol two moles of formaldehyde are produced. Glycerol oxidation with periodate leads to the formation of a mole of formaldehyde and a mole of glycolaldehyde. This last intermediate is further oxidized with the same mechanism to formic acid and another molecule of formaldehyde [26].Following from the above discussion, the oxidation products observed in the presence of Merck TiO_2 have to derive from an •OH-like mediated mechanism, whilst those detected on P25 have to derive, after the rate fall in Fig. 1, from a direct electron transfer of two electrons. The presence of one mechanism on Merck TiO_2 and of two concurrent mechanisms on P25 is evident. On P25 the occurrence of two different types of sites has not to be excluded.

To assess quantitatively the contribution of the two possible mechanisms (OH radical-like vs direct electron transfer), the time profiles of glycerol and its intermediates fully reported in Fig. SI 2–4 have been fitted using the mathematical modelling toolbox PottersWheel [27]. A model based on a specific GLY reaction network reported in Scheme 1, (i.e. on an ODE system) [28] was applied to several data sets at once (multi-experiment fitting), giving the rates reported in Figs. 3–5. The rates on fluorinated TiO_2s are also reported for a later analysis.

The kinetic analysis reveals that for pristine P25 the fall of the rate of GLY disappearance is manly due to the strong fall in GAD (and DHA) production (Figs. 2 and 3). As the total rate is due, according to Scheme 1, to the sum of the rates of intermediate production, below [GLY] = 0.22 mM C3 products are created (and detected, see Fig. SI 3 at 5 and 10 ppm), and above the rate is dominated by GLC + FORM production.

As Fig. 5 reports, the rate of GLC and FORM production on pristine P25 is almost constant with GLY concentration. This is further evidence that the production rate of these compounds depends on the concentration of surface complexes, which is constant after all sites are occupied, and that it is indeed at this complex that the inner sphere electron transfer occurs.

The addition of fluorides to P25 restores the preferential formation of GAD and DHA and depresses the rate of GLC + FORM. This last is further evidence that $C_2 + C_1$ compounds are formed when the surface complex is possible. The observed rate is not null,

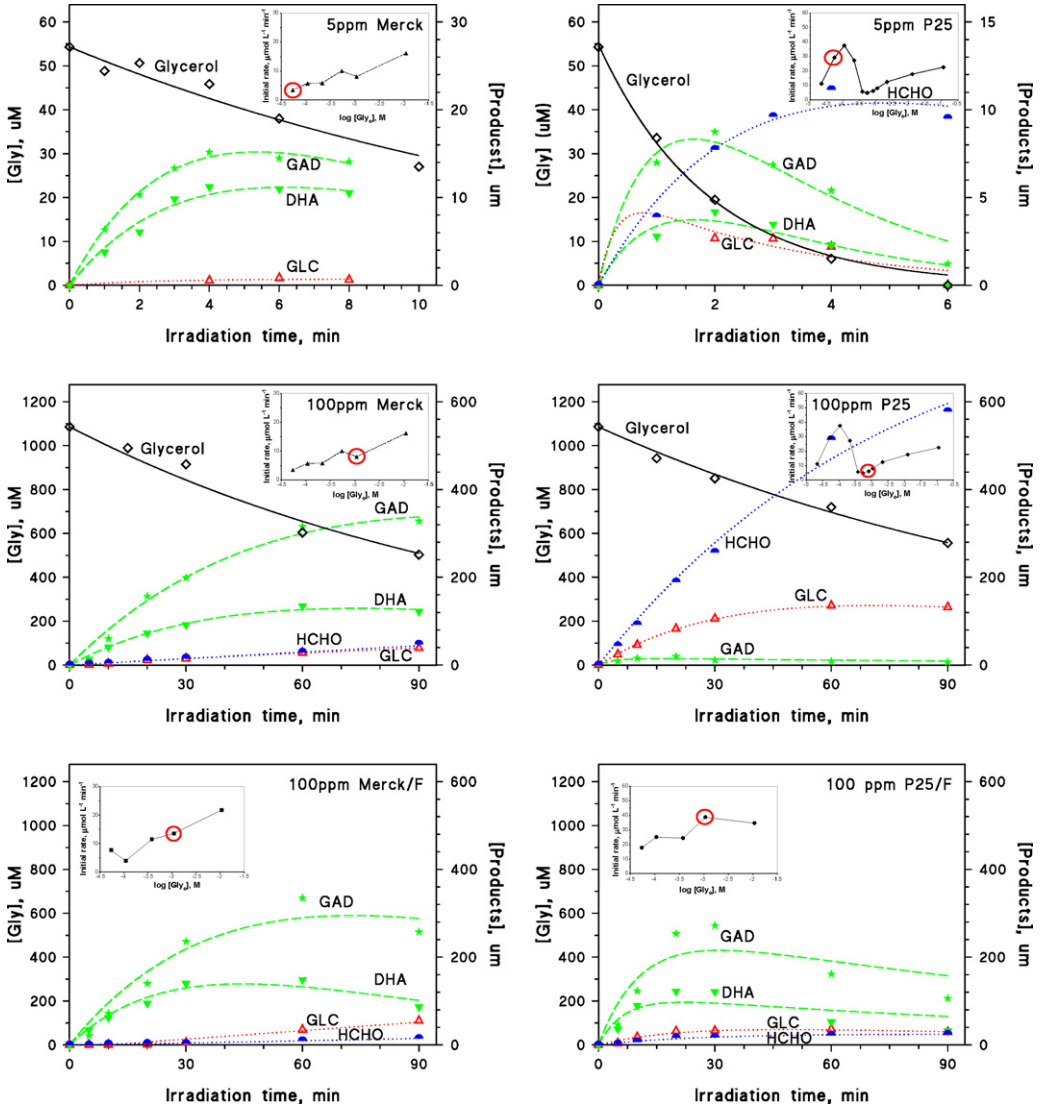

Fig. 2. Comparison of time profiles of intermediates over TiO_2 Merck (left) and P25 (right) (0.5 g L^{-1}) for different initial glycerol concentrations reported in the figures and in the presence of fluorides (bottom). The insets report the reference to the concentration in Fig. 1 in linear/log scale. More extensive time profiles are reported in SI.

indicating that some sites are still available for complexation and are not exchanged with fluoride.

The rate calculated on pristine and fluorinated Merck TiO_2 for GAD, DHA, GLC + FORM are instead almost linear (in the log/log plot). The highest contribution to the GLY disappearance rate is due to the C_3 compounds formation pathway. The disappearance rate of GLY, as well as of GAD and DHA formation follow a dependence on $[GLY]^{0.51}$ both for naked and fluorinated Merck TiO_2. Interestingly, the formation rate of GLC + FORM increases with a higher slope

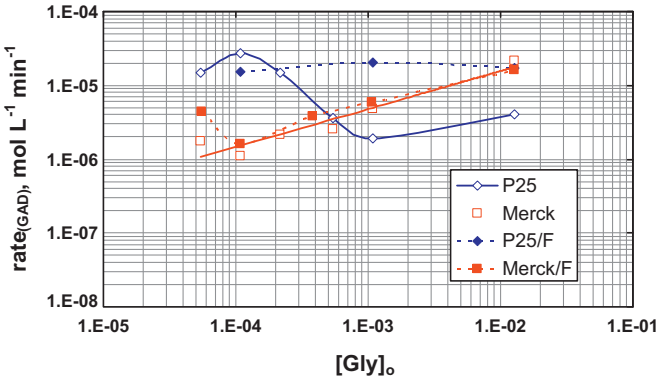

Fig. 3. Rate of GAD formation as a function of glycerol concentration evaluated from the kinetic fit depicted in Scheme 1.

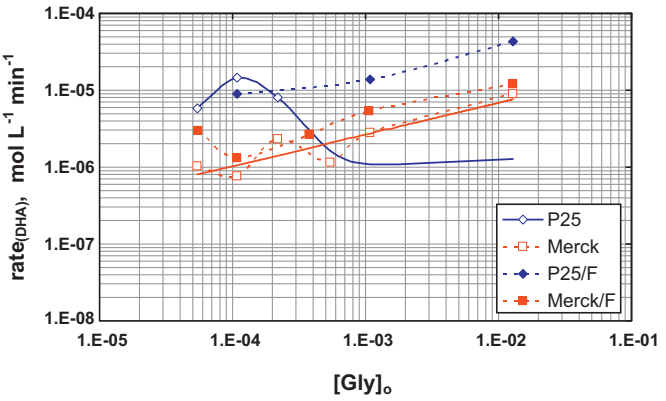

Fig. 4. Rate of DHA formation as a function of glycerol concentration evaluated from the kinetic fit depicted in Scheme 1. The last 3 points on P25 are estimated taking the ratio [GAD]/[DHA] = 1.5 as [DHA] was below the detection limit.

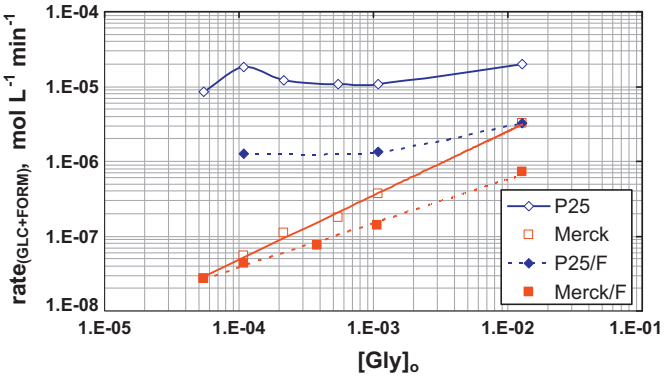

Fig. 5. Rate of GLC + FORM formation as a function of glycerol concentration, evaluated from the kinetic fit depicted in Scheme 1. The rates at 5 and 11 μM for Merck/F have been estimated because [FORM] or [FORM] and [GLC] were below the detection limit.

([GLY]$^{0.86}$ on pristine Merck TiO_2), thus accounting for the observation reported in Fig. SI 4 that some GLC and FORM are present at 1000 ppm [GLY]. This leads to conclude that the two catalysts have sites with different adsorption strength, very large for P25 and weak for Merck TiO_2. For P25, after the rate hill at low [GLY], the rate has a functional dependence on [GLY] as those observed for pristine and fluorinated Merck TiO_2. Thus at least two different sites for electron transfer are present on P25, one strongly complexing, the other acting as trapped OH radical.

The square root dependence on [Substrate] is guessed by a kinetic model (see below and [9]) where charge carrier recombination is allowed, but no back reactions (like $e^- + R^{\bullet+} \rightarrow RH_2$) are considered, irrespective of the actual species involved. Because the back reaction with electrons has to take place at the surface of the catalyst, this indicates that: (a) the GLY oxidation take place in solution where no electrons are available; or (b) back reactions of the type above are not allowed; or (c) electrons are scavenged efficiently and far from the site where oxidation takes place.

The hypothesis (a) was raised to explain the effect of surface fluorination on phenol transformation [6]. Reports on the presence of free OH are conflicting. Serpone et al. reported a fast trapping in some adsorbed state of the OH radicals generated by pulse radiolysis onto the TiO_2 surface [29]. It is argued that the trapped hole and a surface-bound OH radical are indistinguishable species. Jaeger and Bard and recently Schwarz et al. [30,31] reported that by using a spin-trapping method hydroxyl (OH) radicals are present in UV-irradiated TiO_2 aqueous slurries. Nosaka et al. pointed out that the water photooxidation reaction at TiO_2 produced no free OH radical, and spin-trapping agents reacted with surface-trapped holes (adsorbed OH radicals) [32]. The ESR detection of OH radicals on irradiated TiO_2 (anatase) at 77 K was also reported by Anpo et al., although their ESR signals showed no spectral change by H_2O/D_2O exchange [33]. On the other hand, Howe and Graetzel first reported by ESR measurements that photogenerated holes were trapped at lattice O atoms (or Ti—O—Ti sites) at low temperatures of 4.2 or 77 K and did not produce OH radicals [34]. Later Micic et al. confirmed this conclusion and showed clearly that not OH radicals but Ti—O radicals were produced [35]. Ultraviolet photoelectron spectroscopic studies combined with scanning tunnelling microscopy revealed that the O 2p levels for bridging hydroxyls groups (Ti—OH—Ti) at the (1 1 0) face and terminal hydroxyls groups (Ti—OH) at the (1 0 0) face of rutile are both far below the top of the valence band [36,37]. These results are confirmed by theoretical calculations [38]. However, these studies are carried out on clean surfaces in vacuum and could be quite different from the case of a fully hydrated and hydroxylated surface in contact with water.

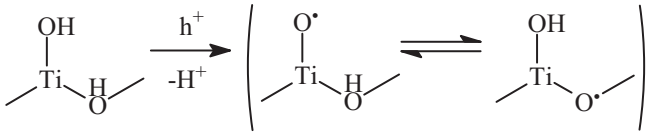

Scheme 2. Pictorial view of the shallow surface trapped hole.

Although the presence of free OH cannot be completely ruled out at least in the presence of fluorination, from the discussion reported above and below on surface oxidizing species we like better to disregard this possibility (after 11 years).

The hypothesis (b) was suggested in the development of DT-IT kinetic model [39] that has some relevance for the interpretation of the present kinetic data as inner sphere electron transfer (ET) is involved for GLY surface complex and outer sphere ET takes place when surface is fluorinated or for the case of Merck TiO_2. For the back reaction by outer sphere mechanism, the rate has been estimated quite low based on the Marcus theory. Apart from the recombination on trapped charge carriers of free electrons and holes, this argument implies that the back reactions with electrons occur only on chemisorbed oxidized radicals. If these cannot be present, as for experimental cases above (competing complexing agent, weak adsorption sites), the rate of the back reaction should be negligible.

Also the hypothesis (c) is supported by some evidence. Electron and hole transfer plausibly occurs at spatially separated sites. It has been demonstrated on both rutile and anatase microcrystals that the reductive and oxidative processes take place on different crystallographic faces [40]. Reductive facets are (1 1 0) and (1 0 1), oxidative facets are (0 1 1) and (0 0 1) for rutile and anatase respectively. It is reasonable to assume that these two processes are not competing for the same surface sites. The presence of distinct sites for oxygen reduction supports the possibility that under complete coverage by ligands (the case of pristine P25) the scavenging of electrons will still be possible. In summary, hypotheses (b) and (c) would apply.

On the oxidative side, the role of direct electron transfer to the hole versus •OH radical-mediated oxidation of organics was strongly debated in the past [7]. Following an analysis of kinetic competition among alcohols and phenol, it was suggested that on naked TiO_2 the oxidation of phenol proceeds for 90% through the reaction with surface trapped hydroxyl radical, the remaining 10% via a direct interaction with the holes, and it was concluded that the trapped hole behaves like •OH (surface bound hydroxyl radical).

From transient absorption studies emerged that at least two kinds of different trap sites exist for holes on the surface: the deep hole and the shallow hole with absorption at 520 nm and around 1200 nm, respectively [41]. Shkrob et al. observed the rapid photooxidation of glycerol by holes on TiO_2 nanoparticles, estimating that half of these holes are scavenged rapidly (in 3.3 ns), the others are scavenged at a slower rate (over 200 ns after the photoexcitation pulse) [42]. The reaction with chemisorbed and physisorbed glycerol may account for the prompt and the slow hole decays, respectively. The shallowly trapped holes are easily excited thermally into the valence band so as to establish equilibrium with the free holes [12], and will therefore have a comparable reactivity and mobility to free holes. The deeply trapped holes are more or less localized at deep traps and exhibit lower oxidizing potential [12,43]. Now, also considering theoretical calculations on rutile, it is accepted that surface ≡Ti—OH groups can act as electron traps but cannot act as hole traps by formation of Ti(IV)(OH•) radicals, as O 2p orbitals of surface ≡Ti—OH are entirely mixed with the O 2p orbitals of the valence band [38].

For the purpose of the present work, a shallow surface hole trap can be schematized as in Scheme 2, where two limiting forms

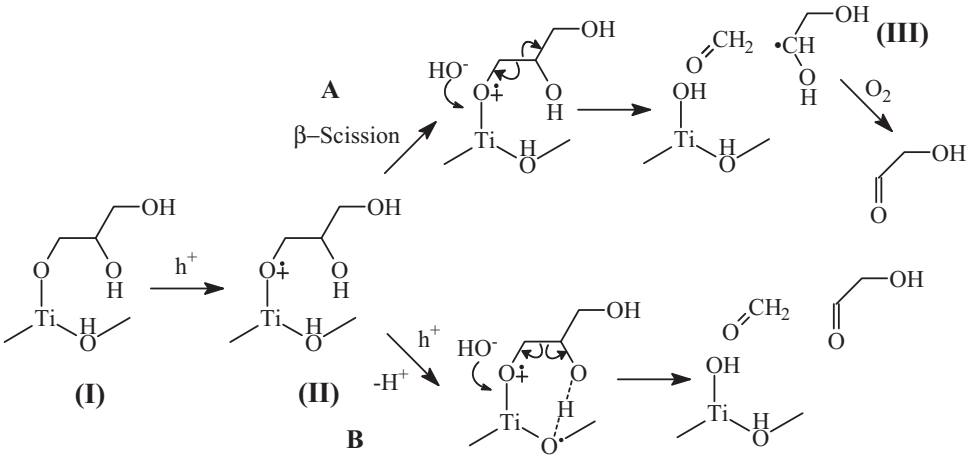

Scheme 3. Mechanism of transformation of the GLY surface complex.

exist. The surface is considered hydrated to avoid to explicitly write charges that depend on the type of crystal face, the type of bridging oxygens, their possible protonation and electron density [44]. The actual hole localization is formally regulated by the ratio K of the right over the left form concentration. The actual electron density distribution of the left and right forms are $1/(1+K)$ and $K/(1+K)$, respectively.

Schematically the species in Scheme 2 will be referred as (Ti(OH)(OH)) → (Ti(O•)(OH)) ⇆ (Ti(OH)(O•)), where the first (OH) refers to linear hydroxy groups and the left (OH) to bridged hydroxy groups. As 3 types of linear hydroxy groups and 3 types of bridged hydroxy groups have been detected [10] on P25, the notation (Ti(OH)(OH)) refers to all of them. It is important to remind that only one type of bridging oxygen is present as (Ti(F)(OH)) on fluorinated P25, and as (Ti()(OH)) on pristine and fluorinated Merck TiO_2. For these cases the notation (Ti(‡)(OH)) will be used.

Following the above discussion, as (Ti(O•)(OH)) is not favoured at acidic pH, K (later referred in Scheme 4 as K_1) will be >1 for naked titania. Recombination will occur by free electrons in CB, on holes that are trapped on titania on both tautomeric forms. Considering fluorinated titania, when terminal hydroxyl is exchanged with fluoride, the left tautomeric form is impeded by the high fluoride electronegativity, and thus $K/(1+K) \approx 1$. In addition, as fluoride is more electronegative than –OH, the radical on bridging oxygen is less stable, i.e. the surface trap is more shallow, and its energy level is more resonant with free holes in the valence band. Free electrons are more stabilized on –Ti(F)– than on –Ti(OH)– and the surface assisted recombination is reduced. Since fluorination increases the rate for substrates that react with OH radicals and depresses the rate for substrates that react by direct electron transfer, the right form performs as adsorbed OH radical. This view reconciles what stated in ref. [6] where shallow traps were indicated with a concise

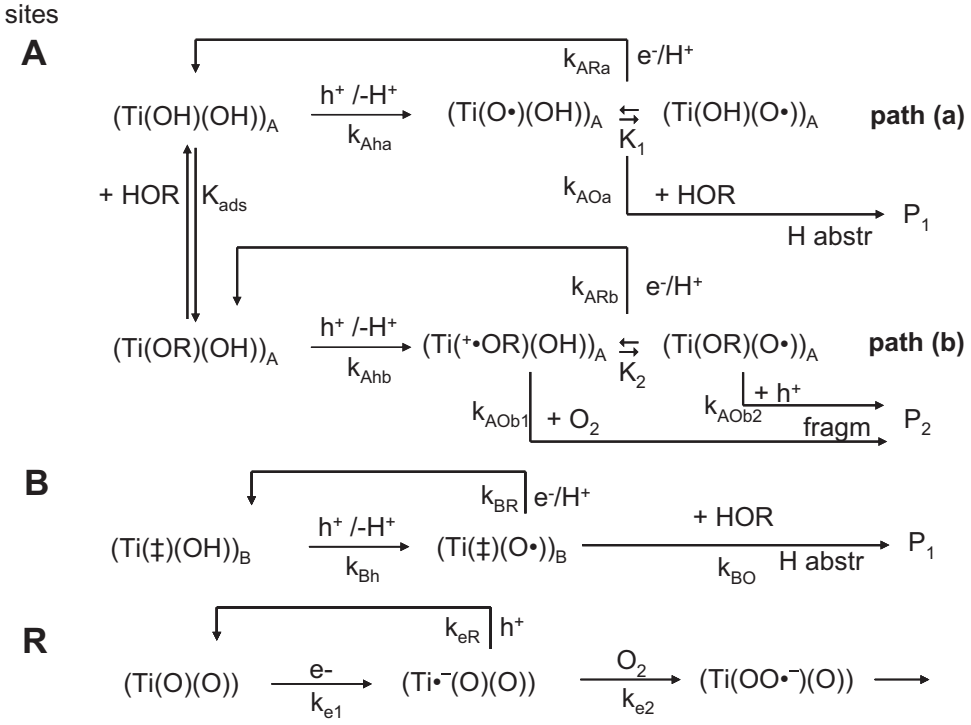

Scheme 4. Kinetic pathways for glycerol transformation on sites A and B together with electron scavenging on sites R. On sites A two pathways (a) and (b) are possible depending on the surface chemical adsorption of the substrate. Products P1 are DHA and GAD, and products P2 are GLC and HCHO.

formalism as (≡Ti—O•), neglecting the resonance form (Ti( )(O•)), and recent reconsideration of surface fluorination [45], where the decrease of the recombination rate concurrent with the increase of the electron transfer rate with reduced dissolved species are invoked to explain the fluoride effect.

Alcohols, and in particular polyols, show good coordinative abilities toward Ti(IV) ions. At suitable concentration GLY is able to occupy surface sites. No information is present in the literature on the structure of the surface complex. If the surface sites with high coordinative ability toward GLY are five-fold coordinated Ti(IV) cations, GLY can act as monodentate ligand. For sake of simplicity the structure I for the surface complex is depicted in Scheme 3. Taking into account the possible presence of surface Ti(IV) with higher coordinative unsaturation (e.g. at steps and kinks), especially on TiO_2 P25, the presence of a chelate surface complex cannot be ruled out. Actually, for the present discussion the exact structure of the complex is irrelevant.

The GLY surface complex I (Ti(OR)(OH)) represents a surface hole trap deeper than Ti(OH)(OH), generating an alkoxyl radical-like species II. Besides being an efficient recombination centre, II has a chemical reactivity very different from the carbon centred radical generated via H-abstraction by the surface adsorbed OH•, namely the Ti(OH)(O•) hole trap. In this case the two produced carbon centred radicals evolve to DHA or GAD.

In order to generate FORM and GLC a second consecutive (monoelectronic) oxidation step on II is needed. Three alternatives can be envisaged to accomplish this: (a) β-scission of the alkoxyl radical-like species II and a subsequent reaction with molecular oxygen of the carbon centred radical formed (pathway A in Scheme 3); (b) a second hole transfer to the vicinal OH group followed by a cleavage of the C—C bond, like in the bielectronic oxidation of diols by periodate (pathway B in Scheme 3); (c) electron injection by the species II in the CB of TiO_2, likewise in the current doubling phenomenon over semiconductor electrodes.

The alternative (c) can be ruled out because (i) electron injection in the CB can be accomplished by carbon-centred reducing radicals, whereas species II is an alkoxyl radical, and as such, it is an oxidant; this conclusion agrees with the evidence that glycerol does not lead to current doubling at TiO_2 electrodes [46].

Concerning the consecutive two-hole transfer, taking into account the radiant power entering in the system ($20\,W\,m^{-2}$ at 360 nm, irradiated area $12\,cm^2$), the concentration of the catalyst ($0.5\,g\,L^{-1}$, 5 mL irradiated suspension volume), and the mean diameter of the particles (30 nm for P25, 80 nm for Merck), there are on average 200/300 photons per particle per second. Considering also the scattering, species II must survive at least tens of milliseconds to have the chance to intercept a second hole. Unimolecular rate constants for the least reactive t-alkoxyl radicals are of the order of $10^{-6}\,s^{-1}$ [47], so are not compatible with the required lifetimes. Then, hypothesis (b) must be discarded.

β-Scission (hypothesis a) is one of the unimolecular processes that alkoxyl radicals undergo, competing with intramolecular H abstraction [47]. Usually the ratio of β-scission to intramolecular H abstraction is low, except for tertiary alkoxyl radicals. It was demonstrated that for vicinal polyols the β-scission yields are very high [48]. This consideration strongly suggests that II evolves via pathway A in Scheme 3, giving FORM and the carbon-centred radical III. The fate of III will be the reaction with molecular oxygen at diffusion controlled rates [47] leading to GLC and hydroperoxides.

Bearing in mind the experimental evidence and the background depicted above, the kinetic framework able to describe the kinetic of glycerol transformation is reported in Scheme 4. It is based on the assumption that there are 2 different types of sites $(Ti(OH)(OH))_A$ and {$(Ti(OH)(OH))_B$ for P25, or $(Ti( )(OH))_B$ for Merck, or $(Ti(F)(OH))_B$ for fluorinated catalysts, all indicated as} $(Ti(‡)(OH))_B$. The sites A are able to chemisorb GLY, as for P25, whilst sites B are not. The species $(Ti( )(O•))_B$ or $(Ti(F)(O•))_B$ are similar to $(Ti(OH)(O•))_A$ but the depth of the shallow traps are manifestly different; this implies that either the recombination reaction constants with free electrons (k_{AR} and k_{BR}) and those for substrate oxidation (k_{AO} and k_{BO}) are markedly different. In particular in the presence of ligands that chemisorb, the deep trapped hole $(Ti(^{+\bullet}OR)(OH))_A$ must recombine free electrons more easily than $(Ti(^{\bullet}O)(OH))_A$ that doubtingly exists owing the above discussion. It is worth noting that the shift of the mechanism from an oxidative attack to GLY (not chemisorbed) mediated by Ti(OH)(O•) shallows surface hole traps, to a direct hole transfer to the surface complex I, leads to very different intermediates (a carbon centred radical and an alkoxyl radical-like species) evolving to different stable products. Crucial for this change in mechanism is the presence of Ti(IV) surface sites with relevant coordinative unsaturation.

According to the preceding discussion, as reducing sites R are not complexing and are not traps for holes (not oxidizing), they are considered separately from sites A. The system of differential equation deriving from Scheme 4 is quite straightforward. The assumption of equilibrium constant-like K_1 and K_2 allows maintaining the different physical information on the 4 different sites for the case A, and concurrently to treat them as 2 couples (a and b) that kinetically have a different performance. The whole recombination constants on path (a) and (b) are $k_{ARa} = (k_{ARa1} + K_1 k_{ARa2})(1 + K_1)$ and $k_{ARb} = (k_{ARb1} + K_2 k_{ARb2})(1 + K_2)$, where k_{ARai} and k_{ARbi} are the reactivity kinetic constants of the limiting forms implied in "equilibrium" described by K_1 and K_2, respectively. The same applies for the oxidation pathways, as $k_{AOa} = (k_{AOa1} + K_1 k_{AOa2})(1 + K_1)$ and $k_{AOb} = (k_{AOb1} + k_{AOb2} K_2)(1 + K_2)$. To simplify the notation, in this case $[(Ti(^{\bullet}O)(OH))_A] + [(Ti(OH)(O^{\bullet}))_A] = A_{ox}$, and $[(Ti(^{+\bullet}OR)(OH))_A] + [(Ti(OR)(^{\bullet}O))_A] = C_{ox}$ (chemisorbed complex). Their respective originating sites are then $[(Ti(OH)(OH))_A] = A_o$ and $[(Ti(OR)(OH))_A] = C_o$. C_o is in equilibrium with sites A_o by $C_o = A_o K_{ads}[HOR]$. Together with the number balance of sites, this last will give a implicit Langmuir isotherm in the system and $C_A = A_o + C_o$. For the non adsorbing sites B the following notation apply: $C_B = [(Ti(‡)(OH))_B]$, $B_{ox} = [(Ti(‡)(O^{\bullet}))_B]$. For the reductive sites R the following notation apply: $C_R = [(Ti(O)(O))_R]$, $R_R = [(Ti^{-}(^{\bullet}O)(O))_R]$. The consequent set of equations in the above notation is:

$$\frac{dA_{ox}}{dt} = k_{Aha}[h]C_A(1 - w_1) - k_{ARa}[e]A_{ox} - k_{AOa}A_{ox}[HOR]; \quad (1)$$

$$\frac{dC_{ox}}{dt} = k_{Ahb}[h]C_A w_1 - k_{ARb}[e]C_{ox} - (w_2[h] + w_3)C_{ox}; \quad (2)$$

$$\frac{dB_{ox}}{dt} = k_{Bh}[h]C_B - k_{BR}[e]B_{ox} - k_{BO}B_{ox}[HOR]; \quad (3)$$

$$\frac{d[h]}{dt} = \Phi_{abs} - [h]C_A(k_{Aha}(1 - w_1) + k_{Ahb}w_1) - w_2[h]C_{ox} - k_{eR}[h][R_R]; \quad (4)$$

$$\frac{d[e]}{dt} = \Phi_{abs} - k_{ARa}A_{ox}[e] - k_{ARb}C_{ox}[e] - k_{e1}[e]C_R; \quad (5)$$

$$\frac{d[R_R]}{dt} = k_{e1}[e]C_R - k_{e2}[O_2][R_R] - k_{eR}[h][R_R]; \quad (6)$$

$$C_{sa} = C_A + A_{ox} + C_{ox} \quad \text{(number balance for sites A where } C_{sa} \text{ are all A sites)} \quad (7)$$

$$C_{sb} = C_B + B_{ox} \quad \text{(number balance for sites B where } C_{sb} \text{ are all B sites)} \quad (8)$$

$$C_{sr} = C_R + R_R \quad \text{(number balance for sites R where } C_{sr} \text{ are all reducing sites)} \quad (9)$$

where $w_1 = K_{ads}[HOR]/(1 + K_{ads}[HOR])$, Φ_{abs} is the absorbed light [9], $w_2 = k_{AOb2}K_2/(1 + K_2)$, $w_3 = k_{AOb1}/(1 + K_2)$, and [h] and [e] are free hole and free electron concentration.

The rate of [HOR] disappearance is given by:

$$Rate_{HOR} = k_{AOa}A_{ox}[HOR] + k_{BO}B_{ox}[HOR] + (w_2[h] + w_3)C_{ox} \quad (10)$$

The full system has only a numerical solution, also under the stationary state hypothesis, as are other complex kinetic systems [39], which gives the rate as a function of many parameters. Besides Φ_{abs}, C_{sa}, C_{sb} and C_{sr} that can be perhaps roughly estimated (but not measured) there are 12 not known kinetic parameters and K_{abs}. A proper simplification of the set of Eqs. (1)–(9) is compulsory. The assumptions $k_{AOb1} = 0$, that implies that the bielectronic transfer is not operating for the β-fragmentation of glycerol, and that in the number balance of sites transient species have negligible contribution, little simplify the solution that remains a complex high order polynomial.

The further possible simplifications under the stationary state assumptions are the following:

(a) there is no pathway (b) for sites A; this means no chemisorption on the surface, so that $w_1 = 0$, no Eq. (2), no C_{ox}, $w_2 = 0$, $w_3 = 0$. This would reflect the case of P25 before the rate fall. It is also assumed that $k_{eR} = 0$ and that $R_R \ll C_{sr}$, that implies that the rate of electron scavenging is primarily due to the reaction with adsorbed oxygen.
(b) there is no pathway (a) for sites A; this means that the only allowed pathway is that with chemisorption, so that $k_{AHa} = 0$, no Eq. (1), $k_{ARa} = 0$, $w_2 = 0$. It is also assumed that $k_{eR} = 0$ and that $R_R \ll C_R$. This returns the rate for P25 just after the fall.
(c) only pathways on site B are considered. This would reflect the case of the rate for Merck TiO_2 and fluorinated catalysts. As for P25 after full surface complexation only sites B are available, this would mirror the case of P25 at the larger [GLY] concentrations, where the rate will sum up to that of case (b) above. As above, it is also assumed that $k_{eR} = 0$ and that $R_R \ll C_R$.

For all the 3 cases, the quantum yield, $\eta = rate/\Phi_{abs}$, is given by a generalized equation as a function of the master variable y:

$$\eta = -y + \sqrt{y(y+2)} \quad (11)$$

At fixed Φ_{abs} the rate is proportional to η. Eq. (11) is identical with that reported (see Eq. (2) in ref. [9]) although the assumption on the separation between oxidative and reductive sites was not previously advised. The simulated rate is reported in Fig. SI 5. A usual Langmuir–Hinshelwood like evolution of the rate as a function of [substrate] is obtained with explicit dependence on catalyst concentration and the absorbed light, without invoking adsorption of the substrate (for cases (a) and (c)). As already outlined [9], for low quantum yield, $\eta = \sqrt{y}$.

The 3 cases above differ for the definition of the master variable y:

$$(a) \quad y_A = \frac{k_{AOa}k_{e2}[O_2]C_{sr}[HOR]}{2k_{ARa}\Phi_{abs}} \quad (12)$$

$$(b) \quad y_C = \frac{w_3 k_{e2}[O_2]C_{sr}}{2k_{ARb}\Phi_{abs}} \quad (13)$$

$$(c) \quad y_B = \frac{k_{BO}k_{e2}[O_2]C_{sr}[HOR]}{2k_{BR}\Phi_{abs}} \quad (14)$$

The case (a) refers to the left of the rate "hill" of P25, because path (a) is applicable only at very low concentration. As at low [GLY] $y_A \to 0$, the rate for case (a) will increase linearly with [GLY] as a series expansion of Eq. (11) demonstrates. For P25 before the rate fall the rate dependence on [GLY] is to a power just smaller than 1, due to the interplay of pathways (a) and (b) in Scheme 4 that is not considered for Eqs. (12) and (13). The rate for case (c) will increase approximately with the square root of the substrate concentration, whilst in the case of full chemisorption the rate is independent on [GLY]. This is evident from the rates for GLY disappearance, as already outlined above for Merck TiO_2 and fluorinated catalysts. For P25 before the "rate fall" the rate is increasing with [GLY], and just after the "rate fall", the rate must be independent. This is not clear from Fig. 1, but is evident from Fig. 5, where the formation rate of GLC + FORM is constant as a function of $[GLY]_o$. Because the formation rate via pathway (b) of GLC + FORM is lower than of formation of C_3 compounds via pathway (a), the comparison of Eq. (12) and Eq. (13) indicates that for P25 the ratio $y_a/y_c = k_{AOa}k_{ARb}[HOR]/(w_3 k_{ARa}) \gg 1$. This point out that $w_3 \ll k_{AOa}$ according with the discussion on β-fragmentation of the adsorbed glycerol, and possibly that also $k_{ARb} > k_{ARa}$, supporting as discussed above that the site at which the adsorption of glycerol takes place $[(Ti(^{+\bullet}OR)(OH))_A]$ is a deeper hole trap than sites $[(Ti(OH)(O^\bullet))_A] + [(Ti(^\bullet O)(OH))_A]$, and that the deep hole trap is a strong recombination site for conduction band electrons.

4. Conclusions

Different TiO_2 specimens have different selectivity toward glycerol transformation. This symmetric molecule when undergoes H-abstraction leads to C_3 oxidized compounds, whilst for direct electron transfer goes through β-fragmentation ($C_2 + C_1$). The first reaction pathway occurs when glycerol is weakly adsorbed and interacts with shallow surface traps. The second pathway is followed when chemisorption on the surface occurs. As the reaction rate in the chemisorbed state is lower than that for H-abstraction, and because the surface complex acts as a deep trap for holes, also the back reaction with free electrons is increased. The experimental evolution of the different products is well explained assuming these simple rules. Due to its peculiar behaviour, glycerol is then a probe for chemical testing the surface of a TiO_2 catalyst due to its ability to perform by an OH radical-like mechanism or, oppositely, by direct hole transfer. Although the primary event of inner sphere electron transfer is very fast, the case of glycerol demonstrated that this could not be beneficial to the photocatalytic efficiency.

Acknowledgement

The authors are grateful to MIUR (co-financed project PRIN2008), and Università di Torino (Ricerca locale) for the financial support.

Appendix A. Supplementary data

Supplementary data associated with this article can be found, in the online version, at doi:10.1016/j.apcatb.2012.02.014.

References

[1] A. Bedini, V. Maurino, M. Minella, C. Minero, F. Rubertelli, J. Adv. Oxid. Technol. 11 (2008) 184–192.
[2] L. Cermenati, A. Albini, J. Adv. Oxid. Technol. 5 (2002) 58–66.
[3] G. Palmisano, V. Augugliaro, M. Pagliaro, L. Palmisano, Chem. Commun. 33 (2007) 3425–3437.
[4] H. Kisch, Adv. Photochem. 26 (2001) 93–143.
[5] G. Martra, Appl. Catal. A: Gen. 200 (2000) 275–285.
[6] C. Minero, G. Mariella, V. Maurino, E. Pelizzetti, Langmuir 16 (2000) 2632–2641.
[7] C. Minero, G. Mariella, V. Maurino, D. Vione, E. Pelizzetti, Langmuir 16 (2000) 8964–8972.
[8] C. Minero, Catal. Today 54 (1999) 205–216.
[9] C. Minero, D. Vione, Appl. Catal. B: Environ. 67 (2006) 257–269.
[10] M. Minella, M.G. Faga, V. Maurino, C. Minero, E. Pelizzetti, S. Coluccia, G. Martra, Langmuir 26 (2010) 2521–2527.
[11] T. Rajh, L.X. Chen, K. Lukas, T. Liu, M.C. Thurnauer, D.M. Tiede, J. Phys. Chem. B 106 (2002) 10543–10548.

[12] D.W. Bahnemann, M. Hilgendorff, R. Memming, J. Phys. Chem. B 101 (1997) 4265–4275.
[13] A.T. Stone, Environ. Sci. Technol. 30 (1996) 1604–1613.
[14] D.F. Ollis, J. Phys. Chem. B 109 (2005) 2439–2449.
[15] A. Mills, J. Wang, D.F. Ollis, J. Catal. 243 (2006) 1–6.
[16] S. Valencia, F. Cataño, L. Rios, G. Restrepo, J. Marín, Appl. Catal. B: Environ. 104 (2011) 300–304.
[17] M. Lewandowski, D.F. Ollis, Appl. Catal. B: Environ. 43 (2003) 309–327.
[18] M. Lewandowski, D.F. Ollis, Appl. Catal. B: Environ. 45 (2003) 223–238.
[19] V. Maurino, C. Minero, G. Mariella, E. Pelizzetti, Chem. Commun. 20 (2005) 2627–2629.
[20] A.P. Reuvers, C.L. Greenstock, J. Borsa, J.D. Chapman, Int. J. Radiat. Biol. Relat. Stud. Phys. Chem. Med. 24 (1973) 533–536.
[21] E.J. Witzemann, J. Am. Chem. Soc. 36 (1914) 2223–2225.
[22] V. Felipe Laurie, A.L. Waterhouse, J. Agric. Food Chem. 54 (2006) 4668–4673.
[23] G.J. Buist, C.A. Bunton, J. Chem. Soc. (1954) 1406–1413.
[24] G.J. Buist, C.A. Bunton, W.C.P. Hipperson, J. Chem. Soc. B (1971) 2128–2142.
[25] G.J. Gainsford, T. Kemmitt, C. Lensink, N.B. Milestone, Inorg. Chem. 34 (1995) 746–748.
[26] D.A. White, D.S. Miyada, R.M. Nakamura, Clin. Chem. 20 (1974) 645–648.
[27] T. Maiwald, J. Timmer, Bioinformatics 24 (2008) 2037–2043, www.potterswheel.de.
[28] ODE system used: $\partial[\mathrm{GLY}]/\partial t = -k_{\mathrm{GLY\ to\ GAD}} \times [\mathrm{GLY}] - k_{\mathrm{GLY\ to\ DHA}} \times [\mathrm{GLY}] - k_{\mathrm{GLY\ to\ GLC+FORM}} \times [\mathrm{GLY}]$, $\partial[\mathrm{GAD}]/\partial t = k_{\mathrm{GLY\ to\ GAD}} \times [\mathrm{GLY}] - k_{\mathrm{GAD\ to\ Other}} \times [\mathrm{GAD}]$, $\partial[\mathrm{DHA}]/\partial t = k_{\mathrm{GLY\ to\ DHA}} \times [\mathrm{GLY}] - k_{\mathrm{DHA\ to\ Other}} \times [\mathrm{DHA}]$, $\partial[\mathrm{GLC}]/\partial t = k_{\mathrm{GLY\ to\ GLC+FORM}} \times [\mathrm{GLY}] - k_{\mathrm{GLC\ to\ Other}} \times [\mathrm{GLC}]$, $\partial[\mathrm{FORM}]/\partial t = k_{\mathrm{GLY\ to\ GLC+FORM}} \times [\mathrm{GLY}] - k_{\mathrm{FORM\ to\ Other}} \times [\mathrm{FORM}]$, where all constants are pseudo first order.
[29] D. Lawless, N. Serpone, D. Meisel, J. Phys. Chem. 95 (1991) 5166–5170.
[30] C.D. Jaeger, A.J. Bard, J. Phys. Chem. 83 (1979) 3146–3152.
[31] P.F. Schwarz, N.J. Turro, S.H. Bossmann, A.M. Braun, A.M.A. Wahab, H.J. Durr, J. Phys. Chem. B 101 (1997) 7127–7134.
[32] Y. Nosaka, S. Komori, K. Yawata, T. Hirakawa, Y.A. Nosaka, Phys. Chem. Chem. Phys. 5 (2003) 4731–4739.
[33] M. Anpo, T. Shima, Y. Kubokawa, Chem. Lett. (1985) 1799–1805.
[34] R.F. Howe, M. Graetzel, J. Phys. Chem. 91 (1987) 3906–3911.
[35] O. Micic, Y. Zhang, K.R. Cromack, A.D. Trifunac, M.C. Thurnauer, J. Phys. Chem. 97 (1993) 13284–13289.
[36] I.M. Brookes, C.A. Muryn, G. Thornton, Phys. Rev. Lett. 87 (2001) 266103.
[37] M.A. Henderson, Surf. Sci. Rep. 46 (2002) 1–308.
[38] C. Di Valentin, G. Pacchioni, A. Selloni, Phys. Rev. Lett. 97 (2006) 166803.
[39] D. Monlor-Satoca, R. Gomez, M. Gonzalez-Hidalgo, P. Salvador, Catal. Today 129 (2007) 247–255.
[40] T. Ohno, K. Sarukawa, M. Matsumura, New J. Chem. 26 (2002) 1167–1170.
[41] T. Yoshihara, R. Katoh, A. Furube, Y. Tamaki, M. Murai, K. Hara, S. Murata, H. Arakawa, M. Tachiya, J. Phys. Chem. B 108 (2004) 3817–3823.
[42] I.A. Shkrob, M.C. Sauer, J. Phys. Chem. B 108 (2004) 12497–12511.
[43] N. Serpone, D. Lawless, R. Khairutdinov, J. Phys. Chem. 99 (1995) 16646–16654.
[44] U. Diebold, Surf. Sci. Rep. 48 (2009) 53–229.
[45] J.F. Montoya, P. Salvador, Appl. Catal. B: Environ. 94 (2010) 97–107.
[46] N. Hykaway, W.M. Sears, H. Morisaki, S.R. Morrison, J. Phys. Chem. 90 (1986) 6663–6667.
[47] K.U. Ingold, in: J.K. Kochi (Ed.), Free Radicals, vol. 1, John Wiley and Sons, New York, 1973, pp. 37–112.
[48] A. Boto, D. Hernandez, R. Hernandez, E. Suarez, J. Org. Chem. 68 (2003) 5310–5319.